Phonon-instability-driven phase transitions in ferroelectric $Bi_2WO_6:Eu^{3+}$: High-pressure Raman and photoluminescence studies

M. Maczka,[1] W. Paraguassu,[2] A. G. Souza Filho,[3] P. T. C. Freire,[3] J. Mendes Filho,[3] and J. Hanuza[4]
[1]*Institute of Low Temperature and Structure Research, Polish Academy of Sciences, P.O. Box 1410, 50-950 Wroclaw 2, Poland*
[2]*Departamento de Fisica, Universidade Federal do Maranhão, São Luis, Maranhão 65085-580, Brazil*
[3]*Departamento de Fisica, Universidade Federal do Ceara, P.O. Box 6030, Fortaleza, Ceara 60455-970, Brazil*
[4]*Department of Bioorganic Chemistry, University of Economics, 53-345 Wroclaw, Poland*
(Received 7 January 2008; revised manuscript received 27 February 2008; published 31 March 2008)

High-pressure Raman scattering and luminescence studies of $Bi_2WO_6:Eu^{3+}$, which is a member of the bismuth layered Aurivillius family of ferroelectrics, are presented. These studies showed the onset of two reversible second order phase transitions near 3.4 and 6.2 GPa. The pressure dependence of Raman bands provides strong evidence that the first phase transition involves the loss of the WO_6 tilt mode around the pseudotetragonal axis. This structural change may be the same as that observed at ambient pressure at 660 °C (from the $Pca2_1$ to $B2cb$ structure). The second phase transition is associated with the instability of a low wave number mode, which behaves as soft mode. The discovery of the soft mode in Bi_2WO_6 that corresponds most likely to the E_u mode responsible for ferroelectricity in Aurivillius family of compounds proves that this transition is of displacive type. Our studies also suggest that the structure above 6.2 GPa is orthorhombic and centrosymmetric and, consequently, the phase transition can be classified as a pressure-induced ferroelectric to a paraelectric phase transition.

DOI: 10.1103/PhysRevB.77.094137 PACS number(s): 77.80.Bh, 78.30.Hv, 77.84.Dy, 78.55.Hx

I. INTRODUCTION

Bismuth layered compounds (Aurivillius family) of general formula $(Bi_2O_2)(A_{m-1}B_mO_{3m+1})$ consist of alternating perovskitelike and fluoritelike layers. The perovskitelike layer may contain 1–8 layers ($m=1-8$).[1] This family of compounds has received much attention for device applications. For instance, these compounds are important candidates for the development of ferroelectric random access memories.[2–4] They also constitute an important class of oxide anion conductors.[1,5]

Bi_2WO_6 is an archetypal $m=1$ member of this family of compounds. It is a well known ferroelectric compound with a high Curie temperature ($T_c \approx 960$ °C) and the largest spontaneous polarization among bismuth layered ferroelectrics.[4,6,7] The room temperature structure is $Pca2_1$.[7] This compound exhibits a second order phase transition at 660 °C to the $B2cb$ structure and a first order phase transition at 960 °C to the $A2/m$ structure.[7] The transition at 960 °C is unique among Aurivillius ferroelectrics because, whereas the other bismuth layered compounds transform at high temperature into the centrosymmetric $I4/mmm$ structure, this prototype tetragonal phase is never reached in Bi_2WO_6.[7] Instead, this material exhibits a reconstructive phase transition into the $A2/m$ structure.[7]

Pressure dependent studies of this family of compounds are scarce and no high-pressure studies have been yet undertaken for Bi_2WO_6. Raman scattering studies under pressure were carried out for $Na_{0.5}Bi_{4.5}Ti_4O_{15}$ and $Bi_4Ti_3O_{12}$, and they showed that these materials exhibited a second order phase transition at about 1.94 and near 3 GPa, respectively.[8,9] These transitions were related to changes in the coordination of bismuth ions and a clear soft mode behavior associated with lattice instabilities was observed.[8,9] The higher pressure phases were assumed to be ferroelectric or antiferroelectric but the mechanisms of the phase transitions were not explained.[8,9] When the pressure increased above 9 GPa, the disappearance of almost all Raman bands was observed for $Na_{0.5}Bi_{4.5}Ti_4O_{15}$.[8] This change was attributed to the pressure-induced amorphization.[8] Amorphization was not observed for $Bi_4Ti_3O_{12}$ but this material exhibited a phase transition near 11 GPa to another phase of unknown symmetry.[9]

In spite of many studies on Bi_2WO_6, very few studies were focused on phonon properties of this material and the understanding of the nature of lattice instabilities in Bi_2WO_6 is still far from being satisfactory. In order to further improve the understanding of the lattice instabilities, it is necessary to access the properties of Bi_2WO_6 both as a function of temperature and pressure. High pressure is a clean probe for investigating the delicate balance between long and short range forces, which in turn should shed light on the lattice instabilities and ferroelectric order. This paper reports studies of $Bi_2WO_6:Eu^{3+}$ single crystal under high pressure through Raman scattering and luminescence of Eu^{3+} ions. The obtained results indicate that Bi_2WO_6 exhibits two structural transformations at about 3.4 and 6.2 GPa.

II. EXPERIMENT

$Bi_2WO_6:2\%Eu^{3+}$ crystals were obtained from Na_2WO_4 flux. The starting melt contained the stoichiometric mixture of Bi_2O_3, Eu_2O_3, and WO_3 corresponding to the $Bi_2WO_6:2\%Eu^{3+}$ compound and the sodium tungstate flux in the molar ratio equal to 3/7 (compound/flux). The reaction mixture was placed in a platinum crucible, heated to 900 °C, kept at this temperature for 10 h, and cooled down to 700 °C at a rate of 1.4 °C/h and to room temperature at a rate of 10 °C/h. The $Bi_2WO_6:Eu^{3+}$ crystals were extracted from the solidified flux by washing with hot water. Since the crystallizing temperature was below the temperature of the

 ©2008 The American Physical Society

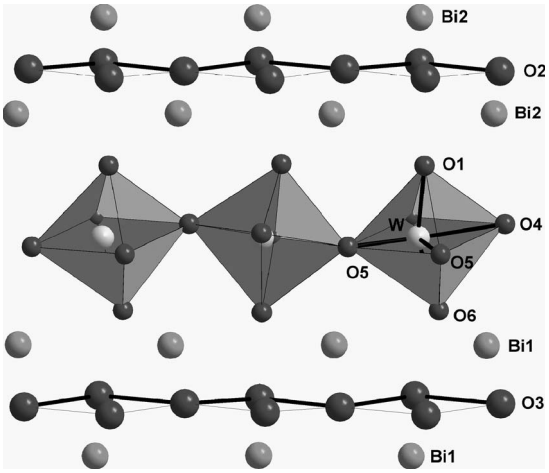

FIG. 1. View of the Bi_2WO_6 crystal structure ($Pca2_1$) along the [101] direction. Orthorhombic *b* axis is perpendicular to the layers.

reconstructive phase transition, the obtained platelike crystals with sizes up to $10\times1\times10$ mm^3 were free of cracks. The crystals have well developed {010} faces. The inspection under polarizing microscope showed that these crystals are single domain. The Bi_2WO_6:Eu^{3+} sample was characterized by x-ray diffraction and its pattern is exactly the same as that obtained for undoped Bi_2WO_6, thus indicating that the very low concentration of Eu^{3+} dopant does not play a fundamental role on the structural properties of the Bi_2WO_6 crystal, and the conclusions obtained in this paper for the doped crystal are also valid for its undoped counterpart.

The high-pressure Raman and luminescence spectra were obtained with a triple-grating spectrometer Jobin Yvon T64000, which is equipped with a N_2-cooled charge coupled device detection system. The 514.5 nm line of an argon laser was used as excitation. An Olympus microscope lens with a focal distance of 20.5 mm and a numerical aperture of 0.35 was used to focus the laser beam on the sample surface. The high-pressure experiments were performed using a diamond anvil cell with a 4:1 methanol:ethanol mixture as the transmission fluid. The spectrometer slits were set for a resolution of 2 cm^{-1}.

III. RESULTS AND DISCUSSION

A. Ambient pressure crystal structure of Bi_2WO_6

In order to understand the general behavior of the Bi_2WO_6 crystal under pressure, it is important to provide a brief discussion of the crystal structure at ambient pressure and room temperature. This crystal is built up of perovskite-like and fluoritelike layers, as shown in Fig. 1. Its room temperature and ambient pressure structure are orthorhombic (space group symmetry $Pca2_1$).[7,10] It can be regarded as derived from a high symmetry body centered tetragonal structure (space group symmetry $I4/mmm$) by condensation of three displacive modes *Bmab*, *Abam*, and *F2mm* (or *Cmca*, *Cmca*, and *Fmm2* in the standard setting) transforming according to the irreducible representations X_3^+, X_2^+, and Γ_5^- of $I4/mmm$.[7,10,11] The distortion of symmetry Γ_5^- (E_u) is responsible for the ferroelectricity in the whole family of Aurivillius compounds and it involves an antiphase displacement of the Bi^{3+} ions and the perovskite blocks along the [110] direction of the tetragonal unit cell plus shift of the tungsten atoms with respect to the oxygen atoms in the perovskite blocks.[6,10] The distortion of symmetry X_3^+ corresponds to the rotation of the rigid WO_6 octahedra along the twofold axis parallel to the polar axis in the orthorhomic phase ([110] direction of the tetragonal phase).[7,10] The condensation of both Γ_5^- and X_3^+ distortions lead to the $B2cb$ structure, which is observed above 660 °C for Bi_2WO_6.[7] Symmetries of the WO_6 and BiO_6 octahedra in the $B2cb$ structure decrease from D_{4h} and C_{4v} to C_2 and C_1, respectively.[7] The distortion of symmetry X_2^+ corresponds to the rotation about the pseudotetragonal axis. For Bi_2WO_6, condensation of the X_2^+ mode occurs upon cooling at 660 °C, leading to the $Pca2_1$ structure and further lowering of the WO_6 symmetry into C_1.[7,10] Moreover, the lowering of symmetry leads to the presence of two nonequivalent sites occupied by Bi^{3+} ions.[7]

B. Luminescence studies

Figure 2 shows the room temperature and ambient pressure luminescence spectrum of Eu^{3+} in this material. We assume that Eu^{3+} ions substitute in this material only Bi^{3+} ions since it is well known that rare earth ions can easily replace the Bi^{3+} ions.[12,13] As can be seen in Fig. 2, the $^5D_0\rightarrow{}^7F_0$ transition gives rise to a single peak at 579.1 nm (17 268 cm^{-1}). The observation of a single line indicates that the energy difference between the $^5D_0$ and $^7F_0$ levels is equal for both sites occupied by Eu^{3+} ions. Therefore, the two sites are nearly identical, which indicates that distortion from the high temperature $B2cb$ structure is very small. The $^5D_0\rightarrow{}^7F_1$ transitions are observed at 586.6 nm (17 047 cm^{-1}), 594.4 nm (16 824 cm^{-1}), and 595.4 nm (16 795 cm^{-1}). The $^5D_0\rightarrow{}^7F_2$ transition gives rise to bands observed at 612.2 nm (16 335 cm^{-1}), 613.4 nm (16 303 cm^{-1}), 616.8 nm (16 213 cm^{-1}), 624.2 nm (16 021 cm^{-1}), and 629.2 nm (15 893 cm^{-1}). The presence of the $^5D_0\rightarrow{}^7F_0$ transition and the *J*-degeneracy splitting indicate that the site symmetry of the Eu^{3+} ions can be described by low symmetry point groups C_1, C_2, C_s, or C_{2v}.[14] This is in agreement with the C_1 symmetry of the Bi^{3+} site established for the orthorhombic phase of Bi_2WO_6 and, consequently, the same site symmetry of Eu^{3+}. In addition to the listed above electronic transitions, the luminescence spectrum shows the presence of a number of weak bands at 580.2 nm (17 236 cm^{-1}), 580.6 nm (17 225 cm^{-1}), 582.1 nm (17 180 cm^{-1}), 583.7 nm (17 132 cm^{-1}), 587.9 nm (17 010 cm^{-1}), 589.7 nm (16 957 cm^{-1}), 591.6 nm (16 903 cm^{-1}), 615.3 nm (16 252 cm^{-1}), and 615.8 nm (16 239 cm^{-1}). The bands in the range of 580–592 nm (17 240–16 890 cm^{-1}) can be attributed to the vibrational sidebands of the $^5D_0\rightarrow{}^7F_0$ transition because the wave number differences between the $^5D_0\rightarrow{}^7F_0$ transition and these weak bands correspond very well to the observed Raman wave numbers. The bands near 615.3 nm (16 252 cm^{-1}) and 615.8 nm (16 239 cm^{-1}) can be most likely assigned to vibronic satellites of the $^5D_0\rightarrow{}^7F_2$ transition.

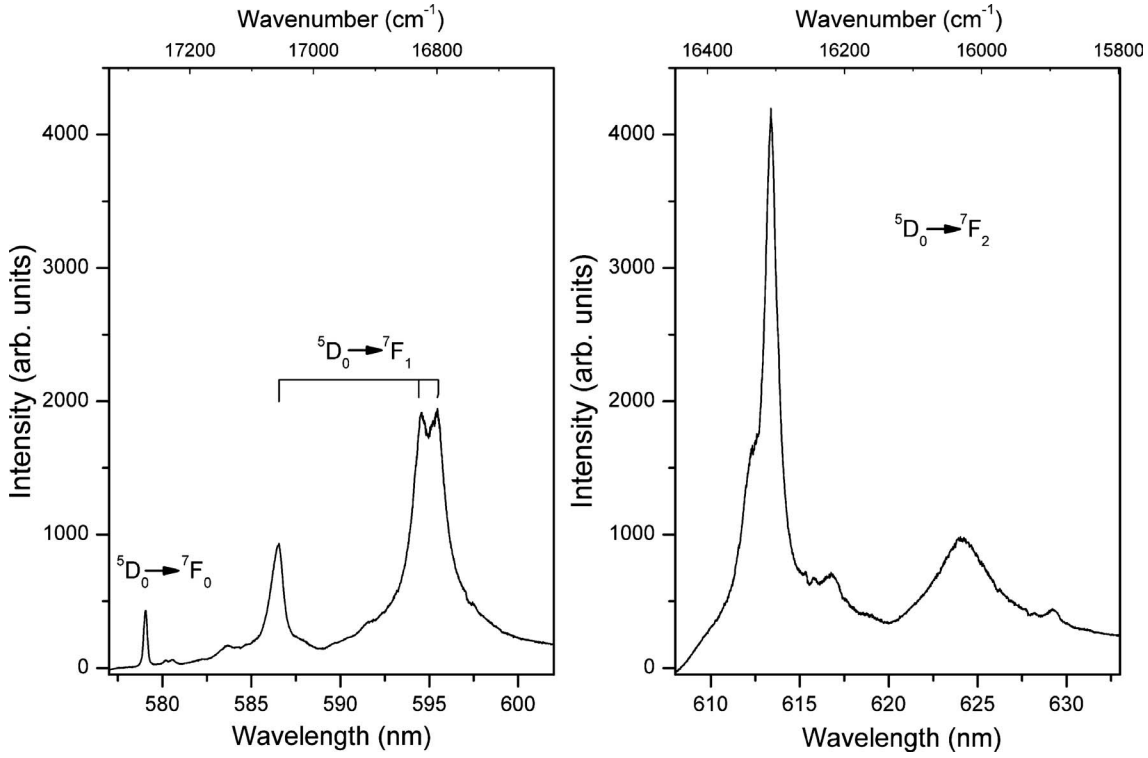

FIG. 2. Room temperature and ambient pressure luminescence spectrum ($^5D_0 \rightarrow {}^7F_{0,1,2}$) of $Bi_2WO_6:Eu^{3+}$.

It is well known that luminescence studies of Eu^{3+} may give insight on the nature of the cation surrounding.[14–18] First of all, the intensity of the $^5D_0 \rightarrow {}^7F_0$ transition can be explained by *J*-mixing effects involving $^7F_0$ and $^7F_2$ levels.[14,16] Our studies show that the integrated intensity ratio of the $^5D_0 \rightarrow {}^7F_0$ and $^5D_0 \rightarrow {}^7F_2$ emissions is 0.014. This ratio is very small, thus indicating weak *J*-mixing effects. Second, it has been shown that the redshift of the $^5D_0 \rightarrow {}^7F_0$ energy from the 17 374 cm^{-1} value calculated for gaseous Eu^{3+} increases with increasing Eu^{3+}-ligand covalency.[14,15] This redshift of −105 cm^{-1} for $Bi_2WO_6:Eu^{3+}$ is smaller than the redshifts found for $Eu_2(MoO_4)_3$ (−144 cm^{-1}), $Gd_2(MoO_4)_3$ (−175 cm^{-1}), or $GdNbO_4$ (−164 cm^{-1}) crystals.[18–20] This result points out to weaker Eu^{3+}-oxygen covalency (weaker crystal field) in Bi_2WO_6 in comparison with the aforementioned compounds. This can be attributed to the fact that Eu^{3+} ions substitute in Bi_2WO_6 the sites occupied by Bi^{3+} ions, which are much larger than Eu^{3+} ions. Third, the covalency and distortion of the Eu^{3+} surrounding also have significant influence on intensity of the $^5D_0 \rightarrow {}^7F_2$ transition, i.e., the ratio between $^5D_0 \rightarrow {}^7F_2$ and $^5D_0 \rightarrow {}^7F_1$ transitions increases with increasing covalency and distortion of the Eu^{3+}-oxygen polyhedra.[14,16,17] This ratio for Bi_2WO_6 is 1.81, which is much smaller than usually observed for other materials with oxygen ligands. For instance, this ratio was 19.3 for Eu_3BWO_9 and more than 4 for titanosilicates.[21,22] This result can be attributed to both weak crystal field strength and relatively weak distortion of the Eu^{3+}-oxygen polyhedra.

The pressure dependent luminescence spectra show that the luminescence bands of Eu^{3+} ions experience redshifts with increasing pressure (see Figs. 3 and 4). Linear fits on the data to $\omega(P)=\omega_0+\alpha P$ give $\omega_0=17\,264.8$ (17 037.8) cm^{-1} and $\alpha=-5.76$ (−10.28) cm^{-1} GPa^{-1} for the $^5D_0 \rightarrow {}^7F_0$ ($^5D_0 \rightarrow {}^7F_1$) electronic transitions. This effect is typically observed for Eu^{3+} ions and it was explained as arising from a much faster downshift of the $^5D_0$ level than the ^7F_j levels upon applying pressure due to the crystal field increase with pressure.[18,23] The pressure dependent spectra also show that the $^5D_0 \rightarrow {}^7F_0$ transition intensity decreases as pressure increases (see Fig. 3). When pressure reaches about 6.2 GPa, the $^5D_0 \rightarrow {}^7F_0$ transition disappears and the observed higher energy component of the $^5D_0 \rightarrow {}^7F_1$ transition becomes very broad. The observed decrease of intensity indicates that Bi^{3+} ions shift under pressure toward the center of bismuth-oxygen polyhedron. In other words, these results indicate that distortion of the bismuth-oxygen polyhedra decreases upon applying pressure. This means that applying pressure at constant temperature may have a very similar effect on the Bi_2WO_6 structure as the increase of temperature at ambient pressure. The disappearance of the band related to the $^5D_0 \rightarrow {}^7F_0$ electronic transition is a strong indication that the crystal undergoes some structural transition to a higher symmetry phase. We investigate these effects by using Raman spectroscopy technique discussed in the next section.

C. Raman scattering studies

A standard group theoretical analysis for the $Pca2_1=C_{2v}{}^5$ room temperature phase of Bi_2WO_6 containing 36 atoms in the unit cell leads to 108 degrees of freedom at the Brillouin zone center (Γ point). The optical modes are

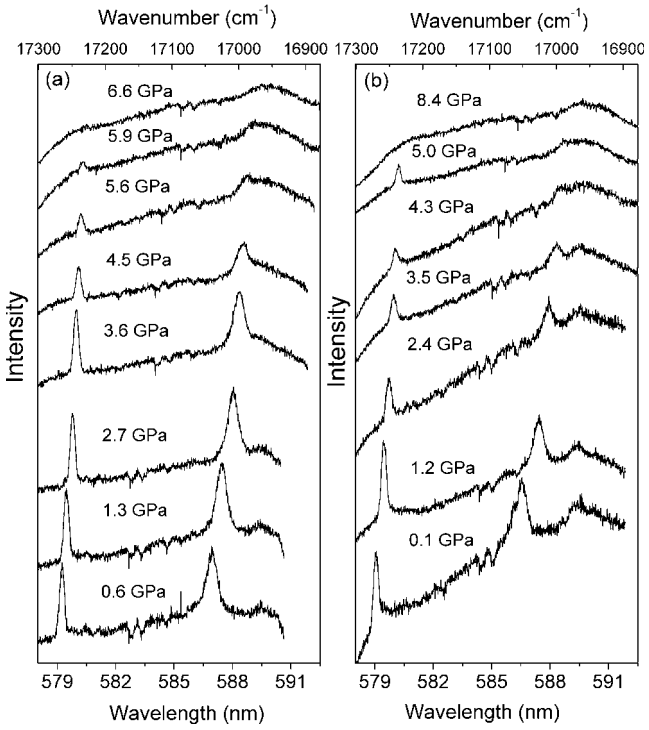

FIG. 3. Part of the luminescence spectra showing pressure dependence of the $^5D_0 \rightarrow {}^7F_0$ transition and higher energy component of the $^5D_0 \rightarrow {}^7F_1$ transition during (a) compression and (b) decompression runs.

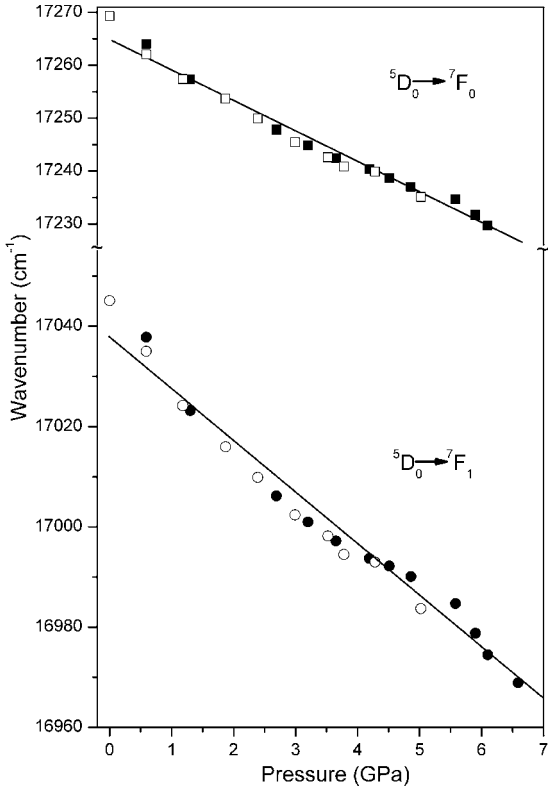

FIG. 4. Plots of the $^5D_0 \rightarrow {}^7F_0$ transition wave number (squares) and the wave number of the higher energy component of the $^5D_0 \rightarrow {}^7F_1$ transition (circles) vs pressure during compression (solid symbols) and decompression (open symbols) runs. The solid lines are linear fits on the data to $\omega(P)=\omega_0+\alpha P$.

distributed among the irreducible representations of the factor group C_{2v} as $26A_1+27A_2+26B_1+26B_2$. Selection rules state that A_1, B_1, and B_2 modes are both Raman and IR active, whereas the A_2 modes are only Raman active. The Raman spectrum at room temperature and near ambient pressure (0.6 GPa) is shown in Fig. 5 (the ambient pressure spectrum is not presented since it is disturbed by a broad luminescence of unknown origin, which disappears upon applying pressure). The number of observed modes is much smaller than expected for the $Pca2_1$ structure because the factor group splitting is very small for the majority of modes. Based on lattice dynamics calculations and polarized Raman and IR studies (not discussed in this paper),[24] the strongest Raman mode at 793 cm^{-1} and the modes in 820–840 cm^{-1} range can be assigned to the symmetric and asymmetric stretching modes of the WO_6 octahedra that involve motions of the apical oxygen atoms (O1 and O6 in Fig. 1) perpendicular to the layers. The modes at 703 and 722 cm^{-1} are due to the asymmetric stretching modes of the WO_6 octahedra, involving motions of the equatorial oxygen atoms (O4 and O5 in Fig. 1) within layers. The bands in the 180–500 cm^{-1} region originate from the bending modes of the WO_6 octahedra coupled with stretching and bending modes of the bismuth-oxygen polyhedra. The modes below 150 cm^{-1} may be assigned to translations of the tungsten and bismuth ions. Lattice dynamics calculations predict that the band observed near 147 cm^{-1} originates from the A_{1g} mode of the tetragonal phase, involving motions of Bi^{3+} ions perpendicular to the layers. Translations of Bi^{3+} ions, corresponding to the E_g mode of the tetragonal phase, and the coupled modes involving motions of both bismuth and tungsten ions within layers, corresponding to the E_u mode of the tetragonal phase, are observed below 105 cm^{-1}.[24] The latter mode has been found to be very important in the Aurivillius structures since it is unstable and triggers the ferroelectric phase transitions.[25]

Once a clear picture of the vibrational properties of Bi_2WO_6 is obtained, we next discuss the effects of hydro-

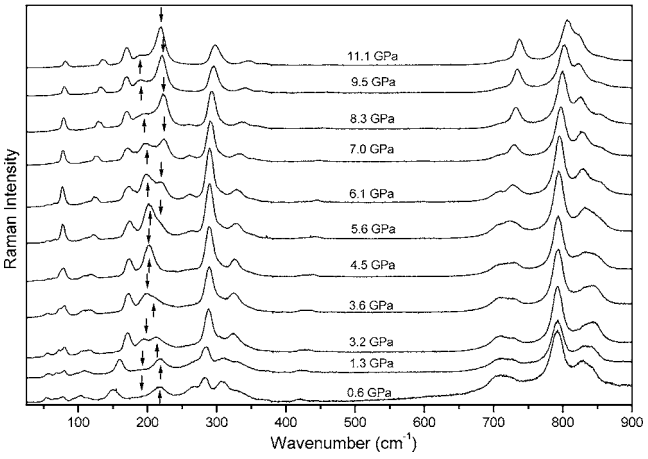

FIG. 5. Raman spectra of Bi_2WO_6 recorded at different pressures during compression experiments. The up and down arrows indicate the modes exhibiting a crossover behavior.

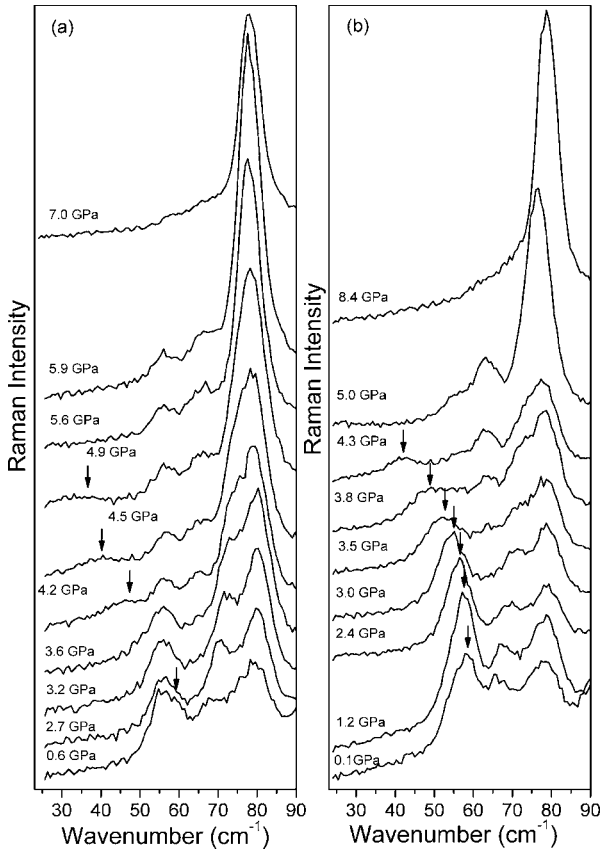

FIG. 6. Low wave number Raman spectra of Bi_2WO_6 recorded at different pressures during (a) compression and (b) decompression experiments. Arrows indicate the soft mode.

static pressure on the structural and vibrational properties of this compound. By increasing pressure, wave numbers of the majority of modes increase (see Figs. 5 and 6). However, some modes exhibit negative pressure dependence. For instance, strongly negative pressure dependence is observed for the 208 cm^{-1} mode (at ambient pressure), which shifts to 192.5 cm^{-1} at 11.1 GPa. As a result of the opposite pressure dependence, the modes at 208 and 186 cm^{-1} exhibit an interesting crossover behavior. Figures 5 and 6 also show that intensities of a number of Raman bands decrease continuously upon increasing pressure. When pressure reaches about 6.2 GPa, the bands observed at ambient pressure near 55 and 92 cm^{-1} disappear. Moreover, the bands at 67 and 78 cm^{-1} coalesce. Another characteristic feature is the appearance of a new band near 65 cm^{-1} (at 3.6 GPa), which disappears near 6.2 GPa. Figure 6 also shows that the band at about 59 cm^{-1}, which is observed on the higher energy side of the stronger 55 cm^{-1} band, exhibits very clear softening upon applying pressure. The band corresponding to the soft mode is weak and broad. Its bandwidth increases significantly upon applying pressure and its wavenumber decreases below 30 cm^{-1} near 5 GPa. Therefore, we could not follow its pressure dependence above 5 GPa. All the observed modifications of the Raman spectra indicate that a continuous transformation takes place in Bi_2WO_6 near 6.2 GPa. By further increasing pressure, intensities of the 835, 260, and 190 cm^{-1} bands continuously decrease and these bands are hardly visible at 11.1 GPa. Moreover, the energy difference between the bands near 793 and 825 cm^{-1} significantly decreases at high pressures. These modifications indicate that Bi_2WO_6 may exhibit another structural transformation above 11 GPa. Unfortunately, we could not follow the pressure dependence of the Raman bands above 11 GPa because of experimental limitations.

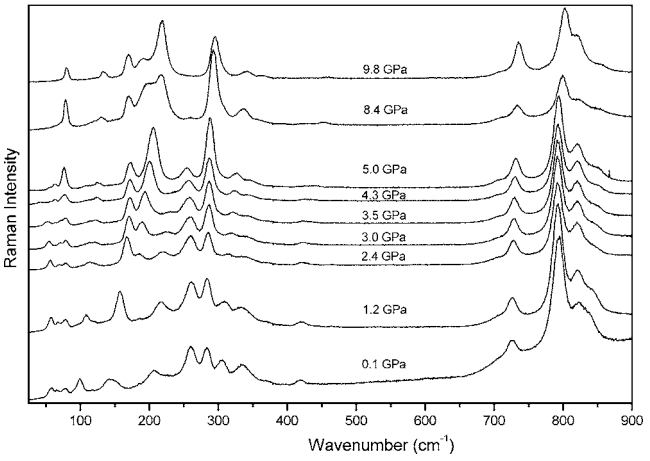

FIG. 7. Raman spectra of Bi_2WO_6 recorded at different pressures during decompression experiments.

In order to get more insight into the mechanism of phase transitions in Bi_2WO_6, we have also performed Raman studies of Bi_2WO_6 crystal during the decompression. Upon releasing pressure, the spectrum of the starting orthorhombic phase was recovered, as can be observed in Fig. 7, thus indicating the reversibility of the process. However, intensities of some bands of the starting phase are different before increasing the pressure and after releasing the pressure. This difference is due to some slight reorientation of the sample during the pressure release and creation of defects in the studied sample. It is interesting to note that due to these changes, the intensity of the soft mode increases, whereas the intensity of the band at 55 cm^{-1} decreases. As a result, the pressure dependence of the soft mode could be more clearly followed in this run (see Fig. 6).

The overall changes in the Raman spectra can be followed by analyzing the wave number (ω) vs pressure (P) plot shown in Fig. 8. This figure shows that the pressure dependence of vibrational modes above 6.2 GPa can be well described using a linear function $\omega(P)=\omega_0+\alpha P$. Below 6.2 GPa, the pressure dependence is more complicated. The totally symmetric mode of the WO_6 octahedra, which is observed at about 793 cm^{-1}, exhibits a wave number decrease as pressure increases up to 3.4 GPa and then a wave number increase above 3.4 GPa. In contrast to this behavior, the modes observed at 835 and 147 cm^{-1} exhibit a wave number increase up to 3.4 GPa, followed by a very weak pressure dependence in the 3.4–6 GPa range. This increase is especially pronounced for the lower wave number band, which shifts from about 147 cm^{-1} at ambient pressure to 171 cm^{-1} at 3.2 GPa. Change in the slope of wave number vs pressure near 3.4 GPa is also observed for a number of other modes (see Table I). These changes indicate that Bi_2WO_6 may ex-

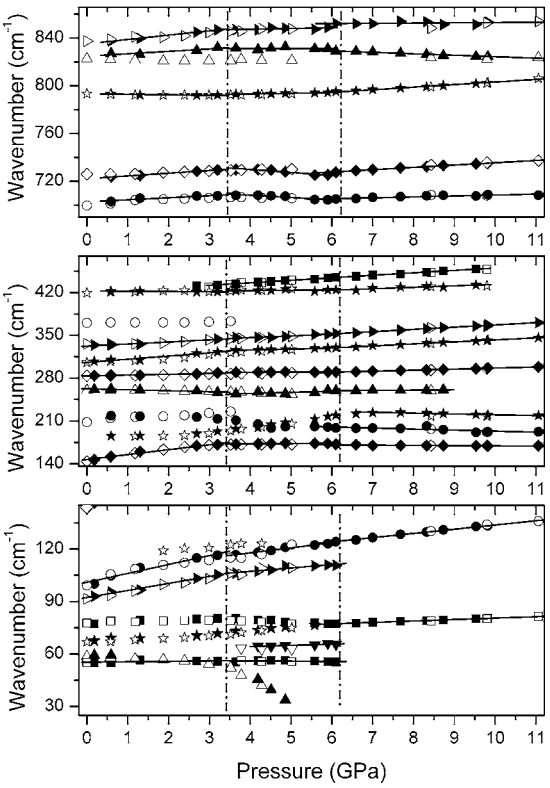

FIG. 8. Wave number vs pressure plots of the Raman modes observed in the Bi_2WO_6 crystal for compression (solid symbols) and decompression (open symbols) experiments. The vertical lines indicate the pressures at which Bi_2WO_6 undergoes phase transitions. The solid lines are linear fits on the data obtained in compression run to $\omega(P)=\omega_0+\alpha P$. Below 6 GPa, the linear fits were not applied for the 209, 182, 76, and 68 cm^{-1} bands as well as the soft mode since for these modes the pressure dependence of wave numbers is nonlinear.

perience near 3.4 GPa a second order phase transition associated with some subtle changes in the crystal structure. Upon further increase of pressure up to 6.2 GPa, very clear coalescence of the 67 and 78 cm^{-1} bands and disappearance of the modes near 55, 65, and 92 cm^{-1} are observed. The most characteristic feature is, however, the significant softening of the mode, which is observed near 59 cm^{-1} at ambient pressure, and its disappearance above 6 GPa. Figure 9 presents the squared wave number of this mode vs pressure. It can be noticed that ω^2 slowly decreases with increasing pressure up to about 3.4 GPa and then quickly decreases above 3.4 GPa. This decrease is linear in both pressure ranges. Linear fit on the data above 3.4 GPa to $\omega^2(P)=\omega_0{}^2+\alpha P$ yields $\omega_0{}^2=6086$ cm^{-2} and $\alpha=998.1$ cm^{-2} GPa^{-1}. The observed mode softens to zero at about 6.1 ± 0.4 GPa, i.e., at approximately the same pressure where some low wave number Raman bands and the $^5D_0\rightarrow{}^7F_0$ luminescence band disappear, and the two low wave number bands coalesce. It is therefore clear that Bi_2WO_6 experiences a structural phase transition at about 6.2 GPa. The observation of the soft mode proves that this transition is of displacive type.

D. Structural changes at the pressure-induced phase transitions

1. Phase transition at 3.4 GPa

In order to obtain information what structural changes occur as a result of the phase transition at 3.4 GPa, it is convenient to shortly discuss what changes in vibrational properties are expected as a result of the orthorhombic distortion of the parent tetragonal phase. First of all, there are only six Raman active modes for the ideal $I4/mmm$ structure of Bi_2WO_6: symmetric stretching mode of the WO_6 octahedra involving motions of apical oxygen atoms (A_{1g} symmetry), bending mode of the WO_6 octahedra involving motions of the equatorial oxygen atoms (E_g symmetry), two internal modes of bismuth-oxygen polyhedra (E_g and B_{1g} symmetry), and two translational modes of Bi^{3+} ions (E_g and A_{1g} symmetry).[26] The transition into the $B2cb$ structure, which is associated with the condensation of the Brillouin zone center and Brillouin zone boundary displacive modes of E_u and X_3^+ symmetries, respectively, leads to doubling of the Bi_2WO_6 formula units in the primitive unit cell and splitting of A_{1g} and B_{1g} modes into A_1+A_2 Davydov doublets and E_g modes into two pairs of Davydov doublets A_1+A_2 and B_1+B_2.[24] Moreover, the IR active modes of the tetragonal phase also become Raman active in the $B2cb$ phase. In the low wave number region, three new modes originating from folding of the acoustic modes into the Brillouin zone center should appear and the unstable E_u and X_3^+ modes could exhibit softening. The phase transition from the $B2cb$ into $Pca2_1$ structure is induced by the condensation of the Brillouin zone boundary X_2^+ mode of $I4/mmm$.[7,11] It also leads to doubling of the Bi_2WO_6 formula units in the primitive unit cell, in comparison with the $B2cb$ structure.[7] As a result, a further splitting of the modes should be observed. For instance, the A_1, A_2, B_1, and B_2 internal modes of the WO_6 octahedra should split into A_1+B_2, A_2+B_1, B_1+A_2, and B_2+A_1 doublets.[24] Our lattice dynamics calculations revealed that splitting between the doublet components is very small for the majority of modes and is not observed in the experimental spectra.[24] Important changes are, however, expected in the low wave number range because some of the modes observed below 120 cm^{-1} may exhibit significant splitting.[24] Moreover, similarly as at the $I4/mmm$ to $B2cb$ transition, three new low wave number modes should appear due to folding of the Brillouin zone boundary acoustic modes and softening of the mode related to the X_2^+ distortion might be observed.

Once we discussed the expected changes of phonon properties as a result of orthorhombic distortion, we move to discuss the possible structural changes in Bi_2WO_6 at the 3.4 GPa transition. First of all, we would like to emphasize that the number of Raman modes observed at 11.1 GPa is much larger than expected for the tetragonal phase mainly because the modes which are IR active in the $I4/mmm$ phase are still observed even at 11.1 GPa. It is therefore obvious that the symmetry of Bi_2WO_6 does not increase to tetragonal up to 11.1 GPa. Since the phase above 6.2 GPa is not tetragonal, it is clear that not all displacive distortions of $I4/mmm$ (X_3^+, X_2^+, and Γ_5^-) are lost as a result of the phase transitions near 3.4 and 6.2 GPa. Since upon heating the X_2^+ mode is lost

TABLE I. Raman wave numbers ω_0 for the three phases of Bi_2WO_6 along with pressure coefficients α obtained from the linear fits on the data to $\omega(P)=\omega_0+\alpha P$. Since the modes at 208, 186, 78, 67, and 59 cm^{-1} have nonlinear pressure dependence in the 0.1–6.2 GPa range, the first column only lists the ambient pressure wave numbers for these modes.

Ambient pressure phase		Intermediate phase		High-pressure phase		
ω_0 (cm^{-1})	α (cm^{-1} GPa^{-1})	ω_0 (cm^{-1})	α (cm^{-1} GPa^{-1})	ω_0 (cm^{-1})	α (cm^{-1} GPa^{-1})	Assignment
835.2	3.6	844.8	0.6	851.1	0.2	WO_6 stretching modes
824.9	2.0	831.3	0.1	836.6	−1.2	
793.3	−0.4	790.4	0.7	781.5	2.2	
722.3	2.2	739.8	−2.5	716.1	1.9	
702.8	1.7	716.2	−1.9	700.6	0.8	
		419.8	4.1	420.4	4.0	WO_6 bending modes + Bi-O stretching and bending modes
422.8	−0.5	422.5	0.2	409.7	2.4	
322.4	3.4	335.1	2.8	330.1	3.7	
305.6	5.2	319.0	1.7	309.5	3.3	
283.6	1.3	288.6	0.2	279.1	1.7	
262.4	−1.6	247.8	1.8	256.6	0.5	
185.8				234.2	−1.4	
208.1				210.4	−1.7	
147.2	8.0	170.7	0.5	173.7	−0.4	Translational motions of Bi^{3+} and W^{6+} ions
101.0	5.1	106.3	2.9	109.7	2.4	
92.3	4.0	99.5	1.9			
77.7				72.2	0.8	
66.9						
		61.4	0.7			
55.4	0.2	56.4	−0.1			
59.3						Soft mode

at the lowest temperature, instability of this mode is weaker than instabilities of the X_3^+ and Γ_5^- modes. It is therefore plausible to assume that this mode is also the first which is lost upon increasing pressure. The anomalies at 3.4 GPa could be therefore most likely attributed to the loss of the octahedral tilt mode around the pseudohexagonal axis (the X_2^+ mode), i.e., to the transition from the $Pca2_1$ to $B2cb$ structure, which is the same as that observed at 660 °C at ambient pressure. If this is true, the dT_c/dP for this transition would be about −188 K/GPa.

2. Phase transition at 6.2 GPa

It is obvious that the phase transition at 6.2 GPa is induced by the instability of the low wave number mode, which is observed as a soft mode in our experiment. Judging from the fact that the soft mode is not observed above 6.2 GPa in Raman spectra, two possibilities can be considered. First, the soft mode is located at the Brillouin zone center but is Raman forbidden in the higher symmetry phase. Second, it is located at the Brillouin zone boundary. The first possibility indicates that the soft mode could be related to the Γ_5^- (E_u) displacive mode of $I4/mmm$. Lost of this mode would lead to the centrosymmetric orthorhombic phase of *Bmab* (or *Cmca* in the standard setting) symmetry.[11] This mode splits into $A_1+A_2+B_1+B_2$ Raman active components in the $B2cb$ phase.[24] However, in the *Bmab* phase, the inversion center is located within the perovskite-type layers and, therefore, the corresponding components are Raman forbidden (they have $A_u+B_{1u}+B_{2u}+B_{3u}$ symmetry). This result would explain the disappearance of the soft mode above 6.2 GPa. Moreover, the B_1, A_2, and B_2 Raman active modes of the $B2cb$ structure, originating from folding of the Brillouin zone boundary acoustic modes of the tetragonal phase into the Brillouin zone center, would also become Raman inactive in the *Bmab* structure. This would explain the disappearance of the three low wave number modes at 55, 65, and 92 cm^{-1}. The second possibility indicates that the phase transition at 6.2 GPa could be related to the loss of the X_3^+ tilt mode. In this case, the symmetry of the phase stable above 6.2 GPa would be orthorhombic $F2mm$. Since the X_3^+ mode is a Brillouin zone boundary mode in the $F2mm$ phase, it cannot be observed in the Raman experiment for this phase. This transition also provides an explanation of the disappearance of some low wave number modes: the three Raman active modes of the $B2cb$ structure, which disappear above 6.2 GPa, could be attributed to folding of the Brillouin zone

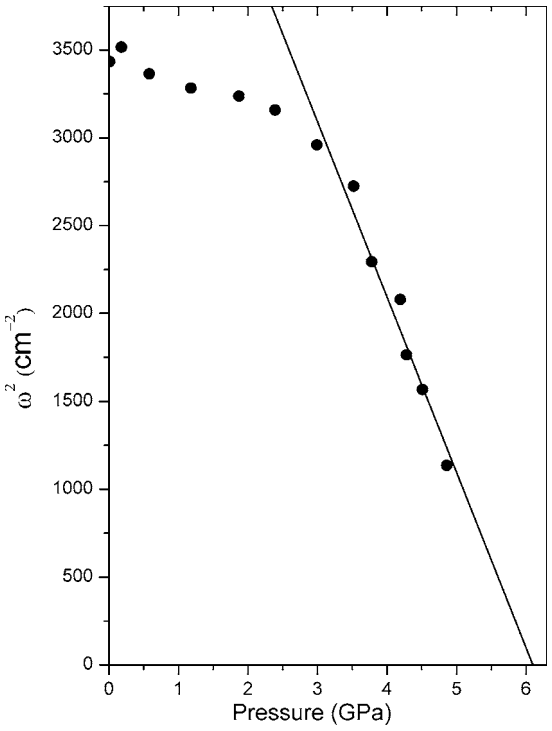

FIG. 9. The pressure dependence of the squared wave number of the soft mode for Bi_2WO_6. The solid line is the linear fit on the data to $\omega^2(P)=\omega_0^2+\alpha P$.

boundary acoustic modes of the $F2mm$ phase into the Brillouin zone center of the $B2cb$ phase.

Although the observed changes in the Raman spectra at 6.2 GPa do not allow to discriminate whether the transition occurs into the *Bmab* or $F2mm$ structure, lattice dynamical calculations and the comparison of the obtained results with the former studies of other Aurivillius compounds provide arguments in favor of the *Bmab* structure. First, the temperature dependent studies revealed the presence of a soft mode for many Aurivillius compounds with $m=2$ ($SrBi_2Ta_2O_9$, $SrBi_2Nb_2O_9$), $m=3$ ($Bi_4Ti_3O_{12}$), $m=4$ ($CaBi_4Ti_4O_{15}$, $SrBi_4Ti_4O_{15}$), and $m=5$ ($Sr_2Bi_4Ti_5O_{18}$).[27–33] Softening of the lower wave number mode was also observed in pressure dependent studies of $Na_{0.5}Bi_{4.5}Ti_4O_{15}$ and $Bi_4Ti_3O_{12}$.[8,9] In all these cases, the soft mode was shown to be related to the polar Γ_5^- (E_u) displacive mode responsible for ferroelectricity and it disappeared at T_c.[8,9,27–33] No soft modes were observed that correspond to the octahedral tilt modes. Although there are no temperature dependent studies reporting the discovery of a soft mode in Bi_2WO_6 or in isostructural Bi_2MoO_6, it is plausible to assume that similarly as in other Aurivillius compounds, the observed soft mode in the present studies also corresponds to the E_u mode. Second, the transition into the *Bmab* phase is consistent with the observed disappearance of the band related to the $^5D_0 \rightarrow {}^7F_0$ luminescence near 6.2 GPa because the loss of the E_u mode requires shifts of the Bi^{3+} ions toward the center of the bismuth-oxygen polyhedra.[6,10] Third, it is in agreement with the slope change in the squared soft mode wave number vs pressure observed near the 3.4 GPa phase transition (see Fig. 9). This transition can be most likely attributed to the loss of the octahedral tilt mode around the pseudohexagonal axis, and, as discussed in literature, the loss of this displacive mode affects little the E_u mode.[7] Fourth, recent lattice dynamical calculations performed for Bi_2WO_6 showed that the E_u mode is unstable and it could appear as a soft mode.[25] Unfortunately, these calculations did not consider instabilities of the Brillouin zone boundary tilt modes. Such calculations are, however, available for another member of the Aurivillius family of compounds, $SrBi_2Ta_2O_9$.[34] They showed that the weakest instability relates to the X_2^+ mode.[34] Experimental data suggest that this is also true for Bi_2WO_6. These calculations also predicted that the instability of the Brillouin zone center E_u mode is weaker than the instability of the Brillouin zone boundary tilt mode corresponding to rotation around the [110] direction of the tetragonal phase (the X_3^- mode for $SrBi_2Ta_2O_9$).[34] It was concluded on that basis that an external pressure would suppress the ferroelectric phase leading to the *Amam* phase and the octahedra tiltings associated with the frozen X_3^- mode would tend to increase under pressure.[34] It is therefore likely that also in case of Bi_2WO_6, the ferroelectric order is suppressed under pressure and the crystal transforms into the *Bmab* phase.

IV. CONCLUSIONS

High-pressure Raman and luminescence studies were performed on Bi_2WO_6 doped with Eu^{3+} ions. These studies revealed that Bi_2WO_6 experiences two second order structural transformations at about 3.4 and 6.2 GPa associated with increasing symmetry. On the basis of the obtained results, we were able to show that the first transition is most likely associated with the loss of the octahedral tilt mode around the pseudotetragonal axis (X_2^+ mode) and the phase symmetry changes from $Pca2_1$ to $B2cb$. This symmetry change is the same as that observed at ambient pressure at 660 °C. The second transition is related to the disappearance of the soft mode that corresponds most likely to the polar E_u mode responsible for ferroelectricity in all Aurivillius-type compounds. In contrast to other members of the Aurivillius family, showing only partial softening of this mode, the wave number of the soft mode observed for Bi_2WO_6 decreases most likely to zero upon approaching the phase transition. This result clearly indicates that the phase transition at 6.2 GPa is displacive. The disappearance of this soft mode at the second phase transition and the observation of some modes which are IR active in the tetragonal phase indicate that Bi_2WO_6 experiences a phase transition to a centrosymmetric orthorhombic phase, most likely of *Bmab* symmetry, not reported at ambient pressure and high temperatures. It is worth noting, however, that centrosymmetric orthorhombic phases were recently discovered at ambient pressure and elevated temperatures for a number of Aurivillius compounds such as $Bi_4Ti_3O_{12}$, $SrBi_4Ti_4O_{15}$, $SrBi_2Ta_2O_9$, $Sr_{0.85}Bi_{2.1}Ta_2O_9$, $PbBi_2Nb_2O_9$, and $PbBi_2Ta_2O_9$.[35–39]

We would like to emphasize that this paper shows the importance of high-pressure studies in this family of materials. Since the soft mode is relatively weak, it could be easily overlooked during the high temperature experiments due to the expected large increase of damping and Rayleigh scatter-

ing. These problems are avoided in high-pressure experiments and, therefore, this weak soft mode is clearly observed, thus allowing to analyze its pressure dependent behavior. We expect that the discovery of the soft mode in Bi_2WO_6 ($m=1$ member of Aurivillius family) will encourage further experimental and theoretical efforts for understanding the origin of lattice instabilities in Aurivillius compounds.

ACKNOWLEDGMENTS

M.M. acknowledges Departamento de Fisica for supporting the visit to UFC. The Brazilian authors acknowledge financial support from CNPq, CAPES, FUNCAP, and FINEP agencies.

[1] M. S. Islam, S. Lazure, R. N. Vannier, G. Nowogrocki, and G. Mairesse, J. Mater. Chem. **8**, 655 (1998).
[2] O. Auciello, J. F. Scott, and R. Ramesh, Phys. Today **51**(7), 22 (1998).
[3] C. A. Paz de Araujo, J. D. Cuchiaro, L. D. McMillan, M. C. Scott, and J. F. Scott, Nature (London) **374**, 627 (1995).
[4] Y. Noguchi, K. Murata, and M. Miyayama, Appl. Phys. Lett. **89**, 242916 (2006).
[5] K. R. Kendall, C. Navas, J. K. Thomas, and H. C. zur Loye, Chem. Mater. **8**, 642 (1996).
[6] A. D. Rae, J. G. Thomson, and R. L. Withers, Acta Crystallogr., Sect. B: Struct. Sci. **47**, 870 (1991).
[7] N. A. McDowell, K. S. Knight, and P. Lightfoot, Chem.-Eur. J. **12**, 1493 (2006).
[8] J. Liu, C. Gao, G. Zou, and Y. Jin, Phys. Lett. A **218**, 94 (1996).
[9] G. A. Kourouklis, A. Jayaraman, and L. G. Van Uitert, Mater. Lett. **5**, 116 (1987).
[10] R. L. Withers, J. G. Thompson, and A. D. Rae, J. Solid State Chem. **94**, 404 (1991).
[11] Yu. E. Kitaev, M. I. Aroyo, and J. M. Perez-Mato, Phys. Rev. B **75**, 064110 (2007).
[12] M. Rico, A. Mendez-Blas, V. Volkov, M. A. Monge, C. Cascales, C. Zaldo, A. Kling, and M. T. Fernandez-Diaz, J. Opt. Soc. Am. B **23**, 2066 (2006).
[13] C. Cascales, A. M. Blas, M. Rico, V. Volkov, and C. Zaldo, Opt. Mater. (Amsterdam, Neth.) **27**, 1672 (2005).
[14] L. D. Carlos, R. A. Sa Ferreira, V. De Zea Bermudez, C. Molina, L. A. Bueno, and S. J. L. Ribeiro, Phys. Rev. B **60**, 10042 (1999).
[15] S. T. Frey, W. De, and W. Horrocks, Inorg. Chim. Acta **229**, 383 (1995).
[16] O. L. Malta, M. A. Counto dos Santos, L. C. Thompson, and N. K. Ito, J. Lumin. **69**, 77 (1996).
[17] E. W. J. L. Oomen and A. M. A. van Dongen, J. Non-Cryst. Solids **111**, 205 (1989).
[18] D. Machon, V. P. Dmitriev, V. V. Sinitsyn, and G. Lucazeau, Phys. Rev. B **70**, 094117 (2004).
[19] M. Buijs, G. Blasse, and L. H. Brixner, Phys. Rev. B **34**, 8815 (1986).
[20] P. Caro, O. K. Moune, E. Antic-Fidancev, and M. Lemaitre-Blaise, J. Less-Common Met. **112**, 153 (1985).
[21] M. Maczka, P. Tomaszewski, J. Stepien-Damm, A. Majchrowski, L. Macalik, and J. Hanuza, J. Solid State Chem. **177**, 3595 (2004).
[22] J. P. Rainho, L. D. Carlos, and J. Rocha, J. Lumin. **87-89**, 1083 (2000).
[23] C. Yuanbin, L. Shenxin, W. Qiuping, and W. Lizhong, Physica B **245**, 293 (1998).
[24] M. Maczka, J. Hanuza, W. Paraguassu, A. G. Souza Filho, P. T. C. Freire and J. Mendes Filho, Appl. Phys. Lett. (to be published).
[25] R. Machado, M. G. Stachiotti, R. L. Migoni, and A. Huanosta Tera, Phys. Rev. B **70**, 214112 (2004).
[26] P. R. Graves, G. Hua, S. Myhra, and J. G. Thompson, J. Solid State Chem. **114**, 112 (1995).
[27] A. Almeida, M. R. Chaves, H. Amorin, M. E. V. Costa, and A. L. Kholkin, J. Phys.: Condens. Matter **17**, 7605 (2005).
[28] J. Liu, G. Zou, H. Yang, and Q. Cui, Solid State Commun. **90**, 365 (1994).
[29] S. Kojima, J. Phys.: Condens. Matter **10**, L327 (1998).
[30] S. Kojima and S. Shimada, Physica B **219**&220, 617 (1996).
[31] S. Kojima, R. Imaizumi, S. Hamazaki, and M. Takashige, Jpn. J. Appl. Phys., Part 1 **33**, 5559 (1994).
[32] S. Kojima, R. Imaizumi, S. Hamazaki, and M. Takashige, J. Mol. Struct. **348**, 37 (1995).
[33] G. Zou, J. Liu, Q. Cui, and H. Yang, Phys. Lett. A **189**, 257 (1994).
[34] J. M. Perez-Mato, M. Aroyo, A. Garcia, P. Blaha, K. Schwarz, J. Schweifer, and K. Parlinski, Phys. Rev. B **70**, 214111 (2004).
[35] R. Macquart, B. J. Kennedy, B. A. Hunter, and C. J. Howard, J. Phys.: Condens. Matter **14**, 7955 (2002).
[36] Q. Zhou, B. J. Kennedy, and C. Howard, Chem. Mater. **15**, 5025 (2003).
[37] C. H. Hervoches, J. T. S. Irvine, and P. Lightfoot, Phys. Rev. B **64**, 100102(R) (2001).
[38] R. Macquart, B. K. Kennedy, B. A. Hunter, C. J. Howard, and Y. Shimakawa, Integr. Ferroelectr. **44**, 101 (2002).
[39] C. H. Hervoches, A. Snedden, R. Riggs, S. H. Kilcoyne, P. Manuel, and P. Lightfoot, J. Solid State Chem. **164**, 280 (2002).